

EFFICIENT ROTATION OF LOCAL BASIS
FUNCTIONS USING REAL SPHERICAL HARMONICSSTEFAN MAINTZ^a, MARC ESSER^a, RICHARD DRONSKOWSKI^{a,b}^aInstitute of Inorganic Chemistry
RWTH Aachen University, 52056 Aachen, Germany^aJülich–Aachen Research Alliance (JARA-HPC)
RWTH Aachen University, 52056 Aachen, Germany*(Received August 25, 2015)*

A well-defined spatial orientation of atomic basis functions is essential for the correct analysis of quantum-mechanical calculations in terms of chemical (bonding) concepts. Here, we present the implementation of a straightforward, convenient algorithm to rotate basis functions using real spherical harmonics within a linear combination of atomic orbitals (LCAO) framework. The highly efficient technique only relies on overlap integrals of the basis functions and Wigner's rotation matrices. To do so, a previously known and simple way to calculate the latter (defined by a rotation axis and angle) for real spherical harmonics is modified to enable chemical-bonding interpretation. The method's usefulness is illustrated by an application to carbon crystallizing in the diamond structure.

DOI:10.5506/APhysPolB.47.1165

1. Introduction

Probably the most common quantum-chemical Ansatz to represent wave functions $\Psi(\vec{r})$ of molecules and also crystals is given by a linear combination of atomic orbitals (LCAO)

$$\Psi(\vec{r}) = \sum_{\mu} C_{\mu} \psi_{\mu}(\vec{r}). \quad (1)$$

By doing so, the wave function is expressed as a sum of certain atomic basis functions $\psi_{\mu}(\vec{r})$ which may adopt any form as long as the basis formed remains complete and covers the entire Hilbert space. In computational practice, however, a complete basis can hardly ever be achieved. Hence, a reasonable, yet flexible form of the basis functions is necessary. There is

a rich atomic-orbital history, and atomic orbitals have shown to be enormously helpful in the quantum mechanics of molecules and crystals [1]. In addition, they provide a perfect starting point for chemical-bonding analysis [2].

With the exception of spherical s functions, atomic orbitals are not invariant to rotations, however. While the ability of a basis to represent a molecular or crystal wave function does not depend on the orientation of its underlying atomic orbitals, the chemical interpretation does. Let us assume the basis functions to be aligned with the axes of the global coordinate system in which a diatomic molecule is described. The coefficients C_μ of Eq. (1) then adopt different values relative to each other whenever the alignment of the bond axis changes, and these coefficients form the core of most bond-analytic tools. It is, therefore, of utmost importance to correctly align the basis functions such as to make chemical-bonding analysis possible.

As will be shown later, a customized basis-function alignment may generally proceed by rotationally transforming spherical harmonics. An exceptionally rigorous and comprehensive review on how to rotate such quantum-mechanical functions was presented by Morrison and Parker [3] based on Euler angles dealing with *complex* spherical harmonics but the use of *real* spherical harmonics is more convenient from a chemical perspective. In 1996, a recursive algorithm to construct rotation matrices for spherical harmonics without detouring via Euler angles was given by Ivanic and Ruedenberg [4]. Twelve years later, in this very journal, Romanowski, Krukowski and Jalbout proposed an algorithm yielding rotation matrices for real spherical harmonics determined only by a single rotation axis and a single rotation angle [5]. This approach not only fits our needs perfectly well but it also offers a simple and computationally efficient way for implementation into existing computer programs.

The aforementioned 2008 contribution deals with the general treatment of real spherical harmonics. To apply their rotation scheme to our representation of atomic orbitals — which is chemical in nature — we must re-define one of their normalization factors [5] for $m = 0$ such that the spherical harmonic is normalized to unity. This is a necessary step for a solid quantum-chemical analysis. Because that very change in normalization carries over to other parts of the theory, we also rigorously re-define all employed mathematical functions, show how the rotation algorithm is implemented in our LCAO framework and present all modified quantities to the community.

2. Definitions

Atomic orbitals or basis functions $\psi_\mu(\vec{r})$ are often defined as a product between a radial part $R(r)$ and a real spherical harmonic $Y_{lm}(\vartheta, \varphi)$

$$\psi_\mu(\vec{r}) = R(r)Y_{lm}(\vartheta, \varphi). \quad (2)$$

Because the radial part is invariant to rotation, one only needs to transform the spherical harmonic upon re-alignment of the entire basis function. The real spherical harmonics $Y_{lm}(\vartheta, \varphi)$ are linear combinations of the complex spherical harmonics $Y_l^m(\vartheta, \varphi)$ such as to make the imaginary parts disappear. That may easily be expressed via

$$Y_{lm}(\vartheta, \varphi) = \begin{cases} -\sqrt{2} \Im(Y_l^m(\vartheta, \varphi)) & : m < 0, \\ Y_l^m(\vartheta, \varphi) & : m = 0, \\ (-1)^m \sqrt{2} \Re(Y_l^m(\vartheta, \varphi)) & : m > 0. \end{cases} \quad (3)$$

Intended as a real instead of complex replacement, however, those linear combinations are required to exhibit the very same mathematical properties as their complex counterparts, given by

$$Y_m^l(\vartheta, \varphi) = \sqrt{\frac{2l+1}{4\pi} \frac{(l-m)!}{(l+m)!}} P_m^l(\cos \vartheta) e^{im\varphi}, \quad (4)$$

using the associated Legendre polynomials

$$P_m^l(x) = \frac{(-1)^m}{2^l l!} (1-x^2)^{\frac{m}{2}} \frac{d^{l+m}}{dx^{l+m}} (x^2-1)^l. \quad (5)$$

Upon following the same route to obtain the Cartesian representation of the real spherical harmonics as before [5, 6], we now arrive at

$$Y_{1,-1} = \sqrt{3/(4\pi)} y/r, \quad (6a)$$

$$Y_{1,0} = \sqrt{3/(4\pi)} z/r, \quad (6b)$$

$$Y_{1,1} = \sqrt{3/(4\pi)} x/r \quad (6c)$$

with $r = \sqrt{x^2 + y^2 + z^2}$. It is compulsory that real spherical harmonics must be normalized to unity, a necessary feature which ensures a reliable probability density of the described electron, and the last set of equations fulfills that criterion. We refrain from showing additional Cartesian representations since these can be looked up in standard textbooks [7, 8]. While the Cartesian representations are not used explicitly in the original algorithm, these non-unity normalizations propagate into the \mathbf{A}^l matrices which have not yet been introduced (see Section 4) but must also be changed accordingly.

3. Rotation of LCAO basis functions

Within the **Lobster** computational framework [9] for chemical-bonding analysis, any crystal wave function $|\Psi_j\rangle$ describing the band j as computed through the projector-augmented wave method [10] is described by local basis functions $|\chi_\mu\rangle$ such as to represent the projected LCAO wave function $|X_j\rangle$. Those basis functions, by their very nature, are aligned to the global coordinate system.

As has been alluded to in Section 1, there will be cases when the projected wave function should be constructed in terms of rotated basis functions $|\chi_\mu^{\text{rot}}\rangle$, however. As a rotation does not affect the completeness of a basis, $|X_j\rangle$ is equal to the wave function represented within the rotated basis $|X_j^{\text{rot}}\rangle$

$$|X_j\rangle = |X_j^{\text{rot}}\rangle = \sum_{\nu} C_{\nu j}^{\text{rot}} |\chi_{\nu}^{\text{rot}}\rangle. \quad (7)$$

We now yield the corresponding set of coefficients $C_{\nu j}^{\text{rot}}$ by a projection technique which is similar to the one used to obtain the original (non-rotated) coefficients $C_{\nu j}$ [9]. To do so, we start with the representation of the non-rotated LCAO wave function and multiply a rotated basis function from the left

$$|X_j\rangle = \sum_{\nu} C_{\nu j} |\chi_{\nu}\rangle, \quad (8)$$

$$\underbrace{\langle \chi_{\mu}^{\text{rot}} | X_j \rangle}_{T_{\mu j}^{\text{rot}}} = \sum_{\nu} \underbrace{\langle \chi_{\mu}^{\text{rot}} | \chi_{\nu} \rangle}_{S_{\mu\nu}^{\text{hyb}}} C_{\nu j}, \quad (9)$$

$$\mathbf{T}^{\text{rot}} = \mathbf{S}^{\text{hyb}} \mathbf{C}. \quad (10)$$

A different way to describe \mathbf{T}^{rot} is found by applying the same technique to Eq. (7)

$$\underbrace{\langle \chi_{\mu}^{\text{rot}} | X_j \rangle}_{T_{\mu j}^{\text{rot}}} = \sum_{\nu} \underbrace{\langle \chi_{\mu}^{\text{rot}} | \chi_{\nu}^{\text{rot}} \rangle}_{S_{\mu\nu}^{\text{rot}}} C_{\nu j}^{\text{rot}}, \quad (11)$$

$$\mathbf{T}^{\text{rot}} = \mathbf{S}^{\text{rot}} \mathbf{C}^{\text{rot}}. \quad (12)$$

By combining Eqs. (10) and (12), we arrive at a matrix equation in which \mathbf{C}^{rot} contains the desired linear-combination coefficients for the rotated basis set

$$\mathbf{S}^{\text{hyb}} \mathbf{C} = \mathbf{S}^{\text{rot}} \mathbf{C}^{\text{rot}}. \quad (13)$$

3.1. Hybrid overlap matrix

To solve matrix Eq. (13), one must find expressions defining the matrix elements for \mathbf{S}^{hyb} and \mathbf{S}^{rot} . Let us begin with the somewhat simpler (hybrid) overlap matrix between a rotated and a non-rotated basis function. By resolving the short-hand notations $\mu = nlm$ and $\nu = n'l'm'$, the hybrid overlap integrals are given by

$$S_{nlm,n'l'm'}^{\text{hyb}} = \int \chi_{nl}^*(r) \chi_{n'l'}(r - R) Y_{lm}^*(\vartheta', \varphi') Y_{l'm'}(\vartheta, \varphi) d^3(r, \vartheta, \varphi). \quad (14)$$

To compute the integral, we first have to transform the rotated spherical harmonic function from the rotated coordinate system — denoted by ϑ' and φ' — to the other (non-rotated) coordinate system. Here, we apply the previously mentioned algorithm [5] which utilizes the spherical harmonics' property of being representable by an expansion over all well-defined but *rotated* spherical harmonics with the same angular momentum l

$$Y_{lm}(\vartheta', \varphi') = \sum_{M=-l}^l Y_{lM}(\vartheta, \varphi) D_{M,m}^l. \quad (15)$$

Let us now assume that the elements of Wigner's rotation matrix \mathbf{D}^l are known and postpone their computation to Section 4. Insertion of the expansion into Eq. (14) yields

$$\begin{aligned} S_{nlm,n'l'm'}^{\text{hyb}} &= \int \chi_{nl}^*(r) \chi_{n'l'}(r - R) Y_{l'm'}(\vartheta, \varphi) \sum_{M=-l}^l Y_{lM}^*(\vartheta, \varphi) D_{M,m}^{l*} d^3(r, \vartheta, \varphi) \\ &= \sum_{M=-l}^l D_{M,m}^{l*} \int \chi_{nl}^*(r) \chi_{n'l'}(r - R) Y_{lm}^*(\vartheta, \varphi) Y_{l'M}(\vartheta, \varphi) d^3(r, \vartheta, \varphi) \\ &= \sum_{M=-l}^l D_{M,m}^{l*} \langle \chi_{nlm} | \chi_{n'l'm'} \rangle. \end{aligned} \quad (16)$$

This final expression yields the hybrid overlap integrals as a short expansion over the original overlap matrix elements $S_{\mu\nu} = \langle \chi_\mu | \chi_\nu \rangle$. In most quantum-chemical cases, these elements will be known (almost) from the very beginning.

3.2. Rotated overlap matrix

Having found \mathbf{S}^{hyb} , there remains only one unknown matrix needed to finally solve Eq. (13). The elements of \mathbf{S}^{rot} , which represent the overlap integrals between two rotated basis functions, are defined by

$$S_{nlm,n'l'm'}^{\text{rot}} = \int \chi_{nl}^*(r) \chi_{n'l'}(r-R) Y_{lm}^*(\vartheta', \varphi') Y_{l'm'}(\vartheta'', \varphi'') d^3(r, \vartheta, \varphi). \quad (17)$$

In addition to one single spherical harmonic that does not belong to the global coordinate system, the second spherical harmonic belongs to a *third* coordinate system denoted by ϑ'' and φ'' . We can essentially apply the same technique that was used towards Eq. (16) but separately for both functions

$$\begin{aligned} S_{nlm,n'l'm'}^{\text{rot}} &= \int \chi_{nl}^*(r) \chi_{n'l'}(r-R) \sum_{M=-l}^l Y_{lM}^*(\vartheta, \varphi) D_{M,m}^{l*} \\ &\quad \times \sum_{M'=-l'}^{l'} Y_{l'M'}(\vartheta, \varphi) D_{M',m'}^{l'} d^3(r, \vartheta, \varphi) \\ &= \sum_{M=-l}^l \sum_{M'=-l'}^{l'} D_{M,m}^{l*} D_{M',m'}^{l'} \\ &\quad \times \int \chi_{nl}^*(r) \chi_{n'l'}(r-R) Y_{lM}^*(\vartheta, \varphi) Y_{l'M'}(\vartheta, \varphi) d^3(r, \vartheta, \varphi) \\ &= \sum_{M=-l}^l \sum_{M'=-l'}^{l'} D_{M,m}^{l*} D_{M',m'}^{l'} \langle \chi_{nlM} | \chi_{n'l'M'} \rangle. \end{aligned} \quad (18)$$

As before, the rotated overlap matrix \mathbf{S}^{rot} is expressed in terms of the original overlap matrix elements. This leaves us with only one unknown matrix in Eq. (13) to be solved using standard linear-algebra methods. As soon as matrix \mathbf{C}^{rot} is used instead of \mathbf{C} (say, for chemical-bonding analyses), one must also use \mathbf{S}^{rot} as the corresponding overlap matrix.

In conclusion, Wigner's rotation matrices must be constructed only *once* in order to re-align the local basis functions. The newly rotated overlap matrix and a helper matrix \mathbf{S}^{hyb} is calculated by short summations over already known overlap integrals. Finally, solving a matrix equation yields the new rotated coefficient matrix such that the basis functions have been efficiently transformed.

4. Wigner's rotation matrices

It has been shown [5, 6] that Wigner's rotation matrices for real spherical harmonics can be split into three matrices \mathbf{B}^l , \mathbf{C}^l and \mathbf{A}^l . While \mathbf{B}^l expresses the real spherical harmonics as a linear combination of canonical polynomials, \mathbf{C}^l rotates the canonical polynomials; finally, \mathbf{A}^l re-expresses

the rotated canonical polynomials as a linear combination of real spherical harmonics. If \mathbf{B}^l is invertible, then $\mathbf{B}^l = (\mathbf{A}^l)^{-1}$ holds and Wigner's rotation matrices for real spherical harmonics are given by

$$\mathbf{D}^l = \left(\mathbf{A}^l\right)^{-1} \mathbf{C}^l \mathbf{A}^l. \quad (19)$$

Since the matrix elements of \mathbf{C}^l for s , p , d and f orbitals are lengthy and already printed in Ref. [6] by Eqs. (13), (18), (32), (35) and (38), we refrain from repeating them. As previously discussed, however, the corresponding matrices \mathbf{A}^l must be modified and are rather simple in structure. As required, all the matrices \mathbf{A}^0 , \mathbf{A}^1 , \mathbf{A}^2 , and \mathbf{A}^3 are invertible:

$$\mathbf{A}^0 = 1, \quad (20a)$$

$$\mathbf{A}^1 = \sqrt{\frac{4\pi}{3}} \begin{bmatrix} 0 & 0 & 1 \\ 1 & 0 & 0 \\ 0 & 1 & 0 \end{bmatrix}, \quad (20b)$$

$$\mathbf{A}^2 = \sqrt{\frac{4\pi}{15}} \begin{bmatrix} 0 & 1 & 0 & 0 & 0 \\ 0 & 0 & 0 & 1 & 0 \\ 1 & 0 & 0 & 0 & 0 \\ 0 & 0 & 0 & 0 & 2 \\ 0 & 0 & 2\sqrt{3} & 0 & 0 \end{bmatrix}, \quad (20c)$$

$$\mathbf{A}^3 = 4\sqrt{\frac{2\pi}{21}} \begin{bmatrix} 0 & 0 & 0 & 0 & 1 & 0 & 0 \\ 0 & 0 & 1 & 0 & 0 & 0 & 0 \\ 0 & 0 & 0 & \frac{\sqrt{6}}{2} & 0 & 0 & 0 \\ 0 & \frac{\sqrt{10}}{20} & 0 & 0 & 0 & 0 & 0 \\ \frac{\sqrt{15}}{5} & 0 & 0 & 0 & 0 & 0 & 0 \\ 0 & 0 & 0 & 0 & 0 & 0 & \frac{\sqrt{15}}{5} \\ 0 & 0 & 0 & 0 & 0 & \frac{\sqrt{10}}{20} & 0 \end{bmatrix}. \quad (20d)$$

5. Application to carbon in the diamond crystal structure

To demonstrate the proficiency of the aforementioned method, we now cover the chemical bonding of carbon in the diamond crystal structure. Its electronic structure and chemical bonding are well-understood and have been covered in the chemical and physical literature [9, 11–13].

The electronic-structure calculations were carried out using standard methods, that is, plane-wave density-functional theory (DFT) in the generalized-gradient approximation (GGA) with the help of the projector-augmented wave (PAW) [10] method as implemented in VASP version 5.3.5

[14–16]. The exchange-correlation energy was approximated using the functional developed by Perdew, Burke, and Ernzerhof [17]. Brillouin-zone integrations were carried out by employing the tetrahedron method with Blöchl corrections [18, 19]. The Brillouin zone was thoroughly sampled with a Γ -centered $23 \times 23 \times 23$ Monkhorst–Pack grid [20]. A plane-wave cutoff of 550 eV served as the convergence criterion.

The extraction of chemical-bonding information from the thus obtained plane-wave (PAW) function was enabled by an analytical projection onto a minimal auxiliary basis made from exponentially decaying contracted Slater-type orbitals [21] as implemented in the **Lobster** program code [9]. Once the projection has been performed, the entire plane-wave electronic structure is re-constructed using local orbitals. This very projection technique has proven its viability in many cases, ranging from amorphous phase-change materials [22] and surface-chemistry problems [23] to very simple ones such as the one at hand, diamond [9]. To extend the tool’s functionality, the previously described rotation algorithm was implemented into **Lobster** in order to get full control over the spatial orientation of the basis set. For demonstration, we start with the reduced diamond unit cell containing two carbon atoms. Figure 1 (a) (left) shows that unit cell in which the included C–C bond axis is part of the yz plane and forms an angle of 45° with the y and z axes of the global coordinate system.

At the beginning, the natural spatial orientation of the local basis set reflects the axes of a Cartesian coordinate system; in other words, the p_z orbital is aligned with the z axis, the p_y orbital with the y axis, and so on. This choice is also implemented in the **Lobster** computer program. For the given crystal structure, however, this leads to a misalignment of the p_z orbitals *in case* these orbitals should serve as the only bond-constructing ones along the direction of the bonding axis, as will be seen shortly. We will now project the Crystal Orbital Overlap Population (COOP) between the two neighboring carbon atoms only using the two neighboring p_z orbitals, and we note that (projected) COOP (or simply pCOOP) is a synonym for an overlap-population weighted densities-of-states which may adopt positive (= bonding), negative (antibonding) and zero (non-bonding) values [24, 25], simply because of the underlying overlap integral between the two neighboring orbitals.

The left part of Fig. 1 (b) shows the chemical bonding of two neighboring carbon atoms for which the non-rotated, non-aligned p_z orbitals have been utilized. The effect of such misalignment is profound because the interactions lowest in energy, approximately between -20 and -10 eV, are non-bonding while there are strongly antibonding (left) interactions just below the Fermi level. Above the Fermi level, in the unoccupied region, we see the first bonding levels (right). Such a scenario is totally unphysical because filled

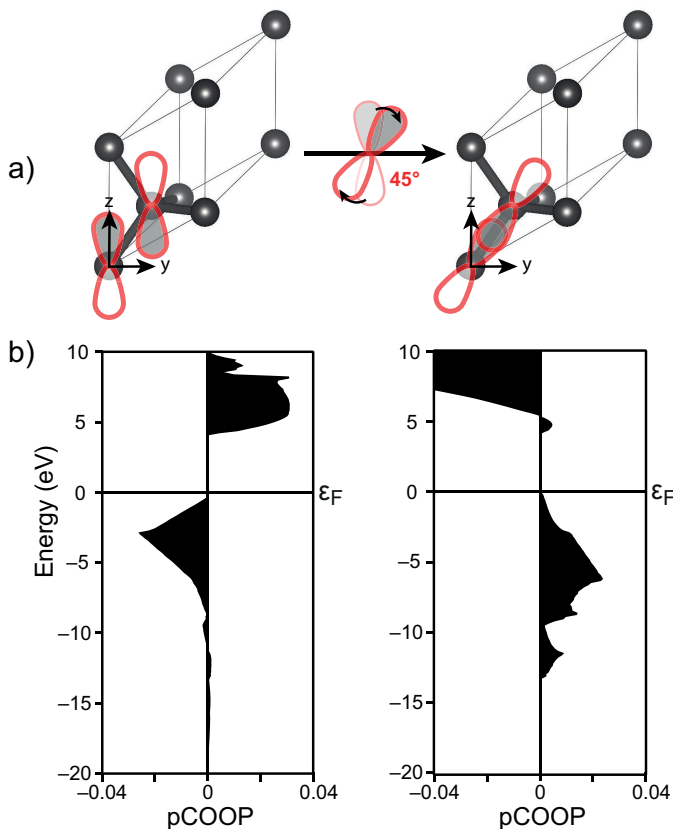


Fig. 1. (a) Illustration of the spatial orientation of the carbon p_z orbitals inside the reduced diamond cell. At the beginning, the p_z orbitals are aligned with the z axis while a 45° rotation around the x axis — pointing at the reader — lets the orbitals align with the bonding axis. (b) pCOOP for the non-rotated (left) and the bond-aligned (right) p_z orbitals. The energy scale has been shifted such that the Fermi level $\varepsilon_F = 0$.

bonding levels are to be expected first, possibly followed by non-bonding levels, eventually followed by antibonding levels in the virtual region. As alluded to already, the reason for the grossly incorrect description lies in the improper alignment of the p_z orbitals as depicted in the left part of Fig. 1 (a) since these are geometrically unable to form such C–C bond.

Nonetheless, Fig. 1(a) (middle and right) also shows how to remedy the improper alignment, namely by a 45° orbital rotation around the x axis such that the p_z orbitals align *exactly* with the C–C bonding axis. As a result, the corresponding pCOOP given in the right part of Fig. 1(b) correctly displays the chemical bonding, namely filled bonding levels in the lower, occupied part and antibonding levels in the upper, virtual part. All formerly antibonding levels in the occupied part below the Fermi level have been eliminated, in harmony with quantum-chemical knowledge [25, 26].

6. Summary

We have demonstrated the importance of a reasonable spatial orientation of an atomic basis set for the proper representation of molecular or crystal wave-functions, for example in the context of chemical-bonding analysis in an LCAO framework. Whenever an atomic-orbital basis must be rotated, this is most conveniently achieved by transforming the real (instead of complex) spherical harmonics part of the basis functions. We have rigorously defined all mathematical functions needed for a straightforward algorithm enabling such rotation, and it only relies on two quantities already known from the unrotated (original) LCAO description of the wave function: the coefficient and overlap matrices \mathbf{C} and \mathbf{S} . The algorithm employs a helper matrix \mathbf{S}^{hyb} and the overlap matrix of the rotated basis functions \mathbf{S}^{rot} , both expressed as a short expansion over Wigner’s rotation matrices. Hence, the coefficient matrix within the rotated basis \mathbf{C}^{rot} can be solved. Wigner’s rotation matrices \mathbf{D}^l for real spherical harmonics are constructed following a slightly modified algorithm which only depends on the selection of a single rotation axis and a single angle.

REFERENCES

- [1] A. Szabo, N.S. Ostlund, *Modern Quantum Chemistry*, McGraw-Hill, New York 1982.
- [2] R.S. Mulliken, *J. Chem. Phys.* **23**, 1833 (1955).
- [3] M.A. Morrison, G.A. Parker, *Aust. J. Phys.* **40**, 465 (1987).
- [4] J. Ivanic, K. Ruedenberg, *J. Chem. Phys.* **100**, 6342 (1996).
- [5] Z. Romanowski, S. Krukowski, A.F. Jalbout, *Acta Phys. Pol. B* **39**, 1985 (2008).
- [6] Z. Romanowski, S. Krukowski, *J. Phys. A: Math. Theor.* **40**, 15071 (2007).
- [7] U. Shmueli (Ed.), *International Tables for Crystallography, Reciprocal Space*, Springer, Dordrecht 2008.
- [8] C.D.H. Chisholm, *Group Theoretical Techniques in Quantum Chemistry*, Academic Press, New York 1976.

- [9] S. Maintz, V.L. Deringer, A.L. Tchougréeff, R. Dronskowski, *J. Comput. Chem.* **34**, 2557 (2013).
- [10] P.E. Blöchl, *Phys. Rev. B* **50**, 17953 (1994).
- [11] D. Glötzl, B. Segall, O.K. Andersen, *Solid State Commun.* **36**, 403 (1980).
- [12] R. Dronskowski, P.E. Blöchl, *J. Phys. Chem.* **97**, 8617 (1993).
- [13] V.L. Deringer, A.L. Tchougréeff, R. Dronskowski, *J. Phys. Chem. A* **115**, 5461 (2011).
- [14] G. Kresse, D. Joubert, *Phys. Rev. B* **59**, 1758 (1999).
- [15] G. Kresse, J. Furthmüller, *Comput. Mater. Sci.* **6**, 15 (1996).
- [16] G. Kresse, J. Furthmüller, *Phys. Rev. B* **54**, 11169 (1996).
- [17] J.P. Perdew, K. Burke, M. Ernzerhof, *Phys. Rev. Lett.* **77**, 3865 (1996).
- [18] O. Jepsen, O.K. Andersen, *Solid State Commun.* **9**, 1763 (1971).
- [19] P.E. Blöchl, O. Jepsen, O.K. Andersen, *Phys. Rev. B* **49**, 16223 (1994).
- [20] H.J. Monkhorst, J.D. Pack, *Phys. Rev. B* **13**, 5188 (1976).
- [21] J.C. Slater, *Phys. Rev.* **36**, 57 (1930).
- [22] V.L. Deringer *et al.*, *Angew. Chem. Int. Ed.* **53**, 10817 (2014).
- [23] V.L. Deringer, R. Dronskowski, *Chem. Sci.* **5**, 894 (2014).
- [24] T. Hughbanks, R. Hoffmann, *J. Am. Chem. Soc.* **105**, 3528 (1983).
- [25] R. Dronskowski, *Computational Chemistry of Solid State Materials*, Wiley-VCH, Weinheim, New York 2005.
- [26] R. Hoffmann, *Solids and Surfaces: A Chemist's View of Bonding in Extended Structures*, VCH, Weinheim, New York 1988.